VILNIUS UNIVERSITY
FACULTY OF PHYSICS
INSTITUTE OF APPLIED ELECTRODYNAMICS AND TELECOMMUNICATIONS

Richard Pinkrah

LOW-FREQUENCY NOISE SPECTROSCOPY OF INFRARED LASER DIODES

FINAL THESIS OF MASTERS STUDIES

Master Final Thesis

Student Richard Pinkrah

Supervisor Assoc. Prof. Sandra Pralgauskaité

Director Prof. Robertas Grigalaitis

Vilnius 2023

Table of Contents

1 Introduction

The first ever laser to be used was built in 1960 by Theodore H. Maiman at Hughes research laboratories. Later in 1962, Robert Hall and a team at General Electric research labs discovered a laser radiating in infrared range from a Gallium Arsenide (GaAs) semiconductor, which was the first-ever semiconductor laser diode with a strange interference pattern implying coherent light emission [1]. Today, semiconductor lasers come in different wavelengths and have become ubiquitous for various applications, including optical storage, medical therapies, image recording, and communication purposes [1]. Lasers produce a significant beam of light oscillating at the same frequency, hence it is named monochromatic, and in phase, therefore emitting coherent light that spreads out very little, even over a long distance. Optical emission of the semiconductor lasers emerges from the radiative recombination of charge carrier pairs in the active region of the device. Electrons in the conduction band recombine with holes in the valence band. This is done by the radiative recombination process, and energy difference is transferred to light. The frequency of the laser radiation is determined by the bandgap of the semiconductor laser material. Large varieties of semiconductor materials have been shown to be suited for semiconductor lasers, and they include GaAs, AlGaAs, GaP, InGaAs, and GaInP.

Recently, the concept of using bismuth with group III to V semiconductors to produce lasers looks innovative in scientific research as it poses a significant reduction of the bandgap and reduces temperature sensitivity [2]. When the band gap is reduced, it is followed by a significant increase in the energy split between the top of the valence band and the spin-orbit band [2]. Today, bismuth semiconductor compound is a good material for optoelectronic such as light sources in the near-infrared region for optical fiber systems [2]. It is foreseen that inclusion of the bismuth to group III to V semiconductor materials results in the realization of very efficient laser diodes, producing longer wavelength, low power consumption, low threshold current, narrow gain spectrum, and high characteristics temperature, which resulted in introducing them in production of quantum well laser structures [2,3]. However, diluting bismuth with GaAs results in other disadvantages which include surface segregation when grown over high temperatures and formation of Bi clusters [3].

The presence of electrical noise in all real semiconductor devices limits their performance [3]. Experiments conducted on semiconductor devices indicate that as the noise in the devices increases, the device tends to have a shorter life span and degrades [4]. Degradation of laser diodes results from an increase in injection current needed for the same light power, which rapidly fail of

the device. Degradation of laser diode is observed when there is a change in its characteristics including response, threshold current, and emitted light intensity. For instance, for laser diodes used for communication purposes, it is very relevant to have a low noise present in the device as it might affect the response or sensitivity of the device. The life span and reliability of semiconductor devices are affected by some other issues in materials which include ohmic contact degradation leading to increase in the operating voltage, packaging process of devices, metal diffusion of electrodes, and heating effects of the active region resulting in enhanced current injection. Owing to the sensitivity of various defects, imperfections and structural non idealities, low-frequency noise of optoelectronic devices is vital as it provides significant information about its quality and reliability [4].

The main goal of this research is to use low-frequency noise (10 Hz – 20 kHz) as a diagnostic tool to measure characteristic of GaAs and GaAsBi based infrared laser diodes with quantum wells between rectangular and parabolic barriers to characterize its performance and reliability.

This work is continuous:

[1] R. Pinkrah, "Low-frequency noise spectroscopy of laser diodes", Report of Scientific Research Work, (2023).

Part of the results of this work were presented in 66th International Conference for Students of Physics and Natural Sciences Open Readings 2023:

[1] R. Pinkrah, S. Pralgauskaité, Low-frequency noise spectroscopy of parabolic quantum well laser diodes", 66th Int. Conf. Open Readings (2023).

2 Overview of Literature

2.1 Infrared Laser Diodes

Infrared laser diode is a high-power laser electronic device that can convert electric current into electromagnetic radiation. These types of lasers emit a wavelength between visible light and microwave radiation. Semiconductor infrared laser diodes are widely used in many applications, which include sensors and optical communication links. Infrared lasers are based on double separate confinement heterostructures with one or several quantum wells (QWs) in the active region. Infrared lasers illustrate a more advanced solution for achieving higher output power of semiconductor lasers and the use of a broadened waveguide, which provides a decrease in internal optical losses and increases quantum efficiency [5]. Sasono and Soetedjo constructed a portable optical tomography apparatus using near-infrared (NIR) laser diode of 904 nm peak spectrum as a light source operating at power 2 mW power for medical diagnosis [6]. The use of 904 nm NIR wavelength allows light to penetrate in the material a bit deeper to allow probing with a low scattering effect. Results showed that the use of laser diode at 904 nm peak spectrum in the NIR region is considerably interesting as this can be used to enhance other optical tomography techniques.

The most established near-infrared lasers, especially those operating at the optical telecommunications wavelength between 1.3–1.5 μm, suffer from intrinsic losses due to non-radiative Auger recombination and inter-valence band absorption [7]. Infrared diode lasers based on group IV-VI compounds play a particularly important role, these laser diodes span a wavelength range from 2.5 μm to about 3.0 μm. Currently, the most commercially available infrared laser diodes are made from IV-VI compounds; this is as a result of lower non-radiative Auger recombination rate in IV-VI compounds as compared to III–V and II–VI materials, high dielectric constant and the resulting weak detrimental influence of defects on non-radiative recombination losses [8].

To ensure a better quality and reliability of operations in these lasers it is very important for us to investigate noise characteristics in these lasers.

2.2 Different Designs of Laser Diodes

Double heterostructure lasers. The double heterojunction laser diode is a type of laser which is based on sandwiching a layer of narrow bandgap material between layers of wide bandgap material. This comprises of the two heterojunctions, as the materials themselves are different and not just the same material with different types of doping. Common materials for double heterojunction laser diode are Gallium Arsenide (GaAs), and Aluminum Gallium Arsenide (AlGaAs). The advantage of the double heterojunction laser diode over other types is that the holes and electrons are confined to the thin middle layer which acts as the active region. By containing the electrons and holes within this area more effectively, more electron-hole pairs are available for the laser optical amplification process [9]. Also, the change in material at the heterojunction helps contain the light within the active region providing additional benefit.

Distributed feedback laser diodes (DFB). Distributed feedback laser diodes are single frequency laser diodes and are used in various forms of telecommunications or data transmission using optical systems operated at very low rates [9]. The active region of the device contains periodically structured elements or diffraction grating [9]. This grating creates a one-dimensional interference, providing optical feedback. Essentially, this process allows only one wavelength to emit from the diode, rather than one center wavelength with a couple of lower power side wavelengths that typically emerges from a standard Fabry-Perot laser diode [9].

Quantum well lasers. Quantum well (QW) lasers are higher-level semiconductor structures compared to the bulk ones in many fields of science and are currently the active medium component in most commercial semiconductor lasers. The structure of quantum well laser is similar to the double heterostructure laser except that the thickness of the active layer in a quantum well is very small, about 10-20 nm [9]. The gain medium in quantum well laser structures consists of one or more layers with thickness consisting of several atomic monolayers [10]. These layers are embedded in barrier material with a larger bandgap that serves to confine the carriers into the wells [10]. Quantum well lasers have been exceedingly successful in a wide range of applications, with optical fiber communications being of very good importance. The basic principle of operation of quantum well lasers are the same as that of bulk lasers. Quantum well lasers require fewer electrons and holes to reach the threshold, which makes the change in dimensions of carrier motion cause improvement in its characteristics. These characteristics include ultra-low threshold current, narrow gain spectrum, and high characteristics temperature [11]. Quantum well lasers with one

active layer are called single-quantum-well (SQW) lasers, and lasers with multiple quantum well are called multi-quantum-well (MQW) lasers. Quantum wells allow the possibility of independently varying barrier and cladding layer compositions and widths, and thus separate determination of optical confinement and electrical injection [11].

Quantum-Wire and Quantum-Dot Laser. The active regions of quantum-wire and quantum-dot lasers are reduced to the de Broglie wavelength regime: 1-D (one dimension-wire) and 0-D (zero dimension-dot). These wires and dots are placed between a *pn* junction. In order to realize such small dimensions, the small active regions are mostly formed by epitaxial regrowth on specially processed surfaces or by a process called self-ordering after epitaxy [12]. The advantages of these lasers are similar to the quantum-well laser. These advantages also stem from their respective densities of states and the densities of states give rise to the optical-gain spectra [12].

Quantum-cascade lasers (QCL). They are manufactured using the same techniques as heterostructure lasers enabling growth of thin layers of semiconductors with great precision and reliability [12]. One advantage relative to the ordinary laser diode is that the radiation wavelength is determined by the structure of the layers instead of the lasing material. QCLs have wavelength limited to approximately 2.5 μm. QCLs operate at much longer wavelengths which include: mid and long-wave infrared production devices up to 11 μm are available, and some 25 μm emitters have been made on an experimental basis [12]. They are used in various applications which include sensors, spectroscopy, medical, scientific, and military applications [12].

2.3 Quantum Structures for Laser Diodes

Quantum structures, also referred to as low dimensional structures, are classified based on the number of reduced dimensions they possess. The dimensionality refers to the degree of freedom posed by the particle [13]. Quantum structures size restricts the movement of carrier charge particles, forcing them into a quantum confinement leading to the formation of discrete energy levels where the carriers exist. Quantum structures are very important for fabrication of laser diodes, light emitting diodes and other optoelectronic devices. Examples of quantum structures confining carries in two, one and zero dimensions are quantum well, quantum wires and quantum dots respectively.

Quantum Wells (QW). Quantum well which is a two-dimensional nanostructure in which there is confinement along one direction and particle is free to move in other two directions.

Particles possess discrete energies associated with the confinement dimensions. Particle energies are continuous along the other two unconfined dimensions.

Quantum wire (QW). This is a one-dimensional nanostructure in which there is confinement along two directions and the particle is free to move in the third direction. Particles have discrete energies associated with these two directions of confinement and continuous along the third unconfinement direction.

Quantum dot (QD). This is a structure in which confinement of particles occurs in all the three directions which results in a zero-dimensional nanostructure. The number of degrees of freedom is zero. Particles have discrete energies associated with its motion along all the three directions.

For these materials to be useful in a device, arrays of quantum wires and quantum dot must be considered, arrays composed of lower band gap material would be embedded in a higher band gap host which leads in the fabrication of laser diode where the active layer is replaced by an array of quantum wire or quantum dot [13]. Gain spectrum narrowing is maximum for the quantum dot. A laser based on a narrower gain spectrum has certain advantages which include lower threshold currents [13-14]. Since fewer carriers are wasted in regions of the spectral space that are not contributing to lasing action. There exists also a significant reduction in the excitation level of the gain medium simply from the reduction of the active layer [14].

2.4 Different Laser Diodes Material Systems

Large varieties of group II–VI semiconductor compounds are frequently used as a basic component for high speed electronic, optoelectronic devices, quantum-well (QW) detectors and laser structures with different concentrations of constituents and impurities. The objective of these structures include reduction in threshold current, improvement of spectral distribution of radiation, greater stability of operation, ease of modulation, and most important lower manufacturing costs [13]. These material systems include GaAs/AlGaAs, GaSbBi/GaSb, InGaSb/GaSb, InGaAs/GaAs and InGaN/GaN.

Scientific research conducted indicated that the use of a series of parallel quantum wires leads to an enhancement of gain in laser diodes [14]. Also, Research conducted on the optical gain spectra and the emission wavelength of $GaSb_{1-x}B_{ix}$/GaSb and traditional $GaAs_{1-x}B_{ix}$/GaAs dilute-bismide quantum wells and wires (QWs, QWRs) showed that the optical gain and the emission wavelength of the GaSb-based QW and QWRs lasers are considerably greater than that of the

traditional GaAs-based QW lasers and QWRs for the same QW, QWR width, Bi content and carrier density [15]. At a high temperature of 300 K, an emission wavelength of about 3 μm with a peak gain of order 3000 cm^{-1} obtained within GaSb-based QWR while for the GaSb-based QWR, a peak gain of order 1800 cm^{-1} is reached providing an emission wavelength at around 1.4 μm [15].

Scientific investigations have also revealed that these material systems consist of very thin active layers epitaxially grown on appropriate substrates. During their growth process, there exist residual stresses in the thin film layer due to the thermal and lattice mismatches between the epilayer and substrate [16-17]. Also, additional stress can be introduced during packaging processes, because of the differences in the thermal expansion coefficients between the chip and heat sink materials [18-19]. These stress affect performance such as the wavelength, threshold, optical gain, and reliability of laser diodes. Furthermore, the energy band structure of group III–V semiconductor materials have been found to change with the lattice mismatch stresses, which result from the variation of the composition of the semiconductor materials [20–21]. The band gap increases when under very high compression and decreases under tension.

It has also been investigated that photoluminescence (PL) and electroluminescence (EL) of GaInAsBi/AlInAs single-QW (SQW) structures grown by the molecular beam epitaxy (MBE) on InP substrates, showed a peak wavelength moving from 2.1 μm to 2.5 μm when the Bi content in the QW layer changes from 5% to ~7% respectively, this shows that a high bismuth content in these material systems increases the peak wavelength of the laser [22].

2.5 Quantum Structures Growth Techniques

There exist various techniques by which quantum well structures are grown, and they include molecular beam epitaxy (MBE), metal-organic chemical vapor deposition (MOCVD) liquid phase epitaxy and vapor phase epitaxy. These growth techniques can achieve a layer thickness control close to about one atomic layer [11]. Over the last decade, new technologies in quantum well materials growth have led to the fabrication of several new functional devices, and performance improvement of these conventional devices, such as lasers, has brought into existence new applications in light wave transmission systems [11].

Molecular Beam Epitaxy (MBE). MBE is a widely used technique for the fabrication of specialized semiconductor devices, which include devices used in optoelectronics and high-frequency applications. The most important aspect of MBE is its deposition rate, which allows

layers to grow epitaxially. MBE is a crystal growth method that is performed using physical adsorption by irradiating the molecular beam in an ultra-high vacuum (UHV) chamber [23]. Since MBE is a high vacuum process, the crystal quality and growth process can be characterized and controlled by real-time monitoring and can form a very abrupt heterointerface [23]. In MBE, beams of atoms or molecules are directed at a heated target crystal. With the presence of UHV conditions, the beams do not interact and can be easily controlled.

Metal Organic Chemical Vapor Deposition (MOCVD). MOCVD was established as a crystal growth technique as a core technology in the late 1980s [24]. MOCVD is a gas phase technique at low pressure [24]. In this method, the depositing of semiconductor film by thermal decomposition of organometallic sources is suitable for the growth of phosphorus compounds and their mass production. MOCVD is also suitable for selective area growth which is essential for realizing high-performance devices and monolithic integration of different types of devices. The constituents are passed as gases (e.g., trimethylgallium and arsine) over a heated substrate, with the resulting composition being controlled by the relative amounts of the appropriate gases [24].

There are some advantages and disadvantages of these growth techniques: In the MBE, the growth of crystals is a result of chemical reactions and not a physical deposition as it exists in the MOCVD. The growth technique of MBE is very good for making low defects and highly uniform semiconductor crystals. It also allows extremely thin layers to be fabricated in a very controlled and precise manner. One major disadvantage of using the MBE growth technique is its cost, it is very expensive. MOCVD growth technique is more economical and potentially flexible, thus allowing you to use more than one component in one stage. Also, one major disadvantage which exists in MOCVD growth technique is its difficulty in producing materials with higher quality features. Table 2.1 summarizes the advantages and disadvantages of the various growth techniques.

Table 2.1 Comparison of different growth techniques

Growth Technique	Advantages	Disadvantages
MBE	Hydrogen free environment Precise control of doping No chemical reaction Quality of layer produced is excellent.	Oval defects are produced. Low throughput Very expensive Low growth rate maintenance
MOCVD	Potentially very flexible with uniform growth of layers Selective growth High throughput	Chemical reactions producing hazardous precursors

There are many different semiconductor materials that can be grown by these techniques, and they have been used to make quantum well structures. Table 2.2 shows a summary of some devices and the growth technique used.

Table 2.2 Application of different techniques for devices

Device	Growth Techniques
Laser diode	MBE, MOCVD
Field Effect Transistors	MBE, MOCVD
Avalanche Photodiode	MBE, MOCVD
Photodiode (PIN)	MBE
Solar Cells	MOCVD

One significant restriction in the use of these growth techniques is that it is important to ensure that the lattice constants which signify how atoms are spaced of the materials to be grown in the heterostructure are very similar [11]. This will help avoid difficulty in retaining a well-defined crystal structure throughout the layers. The growth becomes simplest when the lattice constants are identical. AlGaAs and GaAs have almost identical lattice constants, which helps arbitrary structures to be grown with high quality in this materials system. Another commonly used system is InGaAs with InP; In this case, the proportions of In and Ga are adjusted to give a lattice constant [11].

2.6 Different Designs of Quantum Well Structures

Quantum well structures exist in various designs; these designs are categorized by the shapes in which they exist. They include rectangular or square-shaped and parabolic. QWs are very important because they occupy the active region of the semiconductor laser.

Rectangular Quantum Well (RQW). In the rectangular quantum well, inside the well, energy states are discrete, and particles are free to move outside the well. Inside the quantum well, the particles movement is confined, and the electron wave function penetrates the forbidden barrier, so there is a small probability of seeing the particles outside the well due to tunneling. Penetration of wave function into the barrier is small for the lowest state [25-26].

Parabolic quantum wells (PQWs). The confining potential mimics the well-known harmonic oscillator problem, giving rise to multiple resonant electronic states that could enhance optical non-linearities, which makes an ideal parabolic potential well representing a harmonic oscillator [25-26]. Also, a magnetic field applied to a two-dimensional electron system result in a parabolic potential, and the electrons oscillate at a frequency known as the cyclotron frequency [25].

RQW and PQW are used in light-emitting devices. Rectangular and parabolic quantum well can be produced by the MBE growth technique. In its production, alternate layers of GaAs and AlGaAs of different thicknesses are deposited, increasing the thickness of the AlGaAs layer quadratically with distance, while the thickness associated with the GaAs layer is proportionally reduced [25-26].

The use of Parabolic geometries has brought about many scientific innovations leading to advantages such as equally spaced sub bands, allowing them to act analogous to ubiquitous quantum harmonic oscillators [27]. Owing to the importance of inventing optoelectronic devices including infrared detectors, the use of parabolic QWs has always been very common in many scientific research. For instance, a recent scientific study conducted by Karaliunas et al. demonstrated the high precision design and high-quality growth of GaAs/AlGaAs parabolic QWs using the pulsed analog alloy grading technique [27]. Deimert et al. also reported MBE growth of continuously graded parabolic QW arrays in AlGaAs by varying the Al Cell flux as a function of time [27].

Scientific research also conducted indicated that one main advantage of parabolic quantum wells is their light-emitting properties. Modulating the shape of quantum wells helps in its

distribution in terms of size and composition, which becomes more uniform with parabolic QWs than with rectangular QWs, thereby reducing dislocations and defects in a parabolic quantum well laser, which leads to improving its light-emitting properties [25].

2.7 Noise Sources in Semiconductors

Noise is a spontaneous fluctuation in current and voltage generated in all semiconductor devices. The noise intensity level depends on the life span, fabrication of the device, and operating process of the semiconductor device. Noise is not only a major problem that should be avoided as much as possible. The noise in semiconductor devices can be used as a signal to evaluate and get a more in-depth knowledge of the properties of a particular device [4]. Characterization of low-frequency noise in electronic devices is essential because a noisy system is less reliable and can be rejected for any special purpose [4].

Thermal Noise. Thermal noise, also referred to as Nyquist or Johnson noise, originates from the random thermal motion of electrons in a material. The Brownian motion of charge carriers causes thermal noise. Anytime electrons move, the speed of the electrons becomes random. In this case, more electrons could move in a particular direction with a small net current flow. This net current fluctuates in direction and strength with an average in time equal to zero.

Thermal noise spectral density depends solely on the absolute temperature and ohmic resistance of the device under investigation and can be expressed by the Nyquist formula [28]:

$$S_u = 4kTR; \qquad (1)$$

where $k, T,$ and R represent Boltzmann's constants, temperature, and device resistance.

Thermal noise exists in every resistor and resistive part of a device and sets the lowest limit on the noise in an electric circuit. The thermal noise spectrum is constant in this case it does not depend on frequency. Since thermal noise cannot be neglected and is found in all devices and the resistive part, its intensity depends on temperature and resistivity, it is often used as a reference for noise measurement system calibration.

Shot Noise. A second fundamental source of noise is shot noise. It describes plate current noise resulting from random fluctuations in electron emission from cathodes in a vacuum tube. This analogy was made with the effect of a lead shot from a gun striking a target. Shot noise also occurs in semiconductor devices, releasing carries into the potential barrier region. An example is what occurs in the *pn* junction diode. The spectrum of the fluctuation current is white and is

proportional to the elementary charge q of the carriers and the average current I, and it is expressed by the formula [4]:

$$S_I = 2qI; \qquad (2)$$

where q, I represent the charge of an electron and current, respectively.

The current flowing across a potential barrier, for instance, the one in the *pn* junction is not continuous due to the discrete nature of electrons. Shot noise with very low applied current levels is useful for detecting parasitic shunt resistors across a photodiode [4]. Shot noise can be used for diagnosing photodiodes, Zener diodes, Avalanche diodes, and Schottky diodes [4].

Generation-recombination noise (GR) noise in semiconductors is caused by fluctuations in the number of charge carriers due to the generation and recombination process [4]. Some electrons receive sufficient energy from thermal lattice vibrations to get a release from the valence band, thus generating charge carriers simultaneously. A reverse process also occurs, in which electrons from the conduction band jump to the valence band by releasing some energy. Electronic states within the forbidden bandgap are referred to as traps and exist due to various defects or impurities in the semiconductor or at its surfaces. Since traps cannot be avoided, but a semiconductor device can be free from GR noise at certain temperature ranges this is because of energy level being far below or above the Fermi level, and hence communication with such a kind of trap becomes negligible [4]. The spectral density of generation recombination noise can be expressed below:

$$S_I(f) = 4I_o^2 \cdot \frac{\Delta N_0^2}{N_0^2} \cdot \frac{\tau_0}{1+(w\tau_0)^2}; \qquad (3)$$

where I_0 and τ_0 represent average currents and relaxation time of carriers, respectively, and ΔN_0^2 and N_0^2 represent the variance of fluctuating number of charge carriers and the number of charge carriers in conduction bands, respectively.

At low frequencies, ($w\tau_0 \ll 1$) GR noise has a constant spectrum, and at high frequencies ($w\tau_0 \gg 1$), it is inversely proportional to the frequency squared. Generation and recombination noise is frequently negligible in high-quality silicon devices, due to the presence of lattice defects, it is noticeable in heterostructure and compound semiconductors [4].

1/*f* noise. 1/*f* noise, also referred to as flicker noise or excess noise, is present in many basic systems [29]. An important feature of this type of noise is the presence of contributions from processes over a wide range of frequencies and appears to have the same properties at any time scale, thus it being time invariant [30]. At low frequencies, 1/*f* types of noise occur. Spectrum density increases as the frequency decreases and vice versa. High frequencies above 100 Hz or 1 kHz are marked by other types of noise, including thermal noise or generation recombination noise [29]. 1/*f* noise is present in all biased semiconductor devices. This noise usually corresponds with material failures or imperfection during the fabrication process. Most research conducted concludes that this noise exists at very low frequencies up to 10^{-6} Hz [30].

In electrical devices, flicker noise is a consequence of random current or voltage fluctuations due to the instability of electrical resistance or other device characteristics of the system [29]. In this case, 1/*f* noise results from fluctuations in carrier density, Fluctuations in carrier density cause fluctuations in the conductivity of the material. This produces a fluctuation of voltage drop when a direct current flows. Voltage is referred to as the flicker noise voltage. The mean square value is proportional to the square of the direct current flowing. The power spectral density of voltage 1/*f* noise is inversely proportional to current squared, which is inversely proportional to the total number of mobile charge carriers in the semiconductor device. It is expressed mathematically by:

$$\frac{S_u}{U^2} = \frac{S_i}{I^2} = \frac{S_r}{R^2} \sim \frac{1}{N}; \qquad (4)$$

This noise is however used to model fluctuation of device parameters with time [30]. The 1/*f* noise can be described as a superposition of generation and recombination noise sources which is the simplest way to obtain its characteristics, with relaxation times distributed widely, which can be shown in Fig. 2.1 and expressed mathematically as

$$\frac{S_u}{U^2} = \sum_i \frac{a_i \tau_i}{1 + w^2 \tau_i^2}; \qquad (5)$$

where a_i, τ_i represent a dimensionless value that describes the intensity of relaxation noise and relaxation times, respectively.

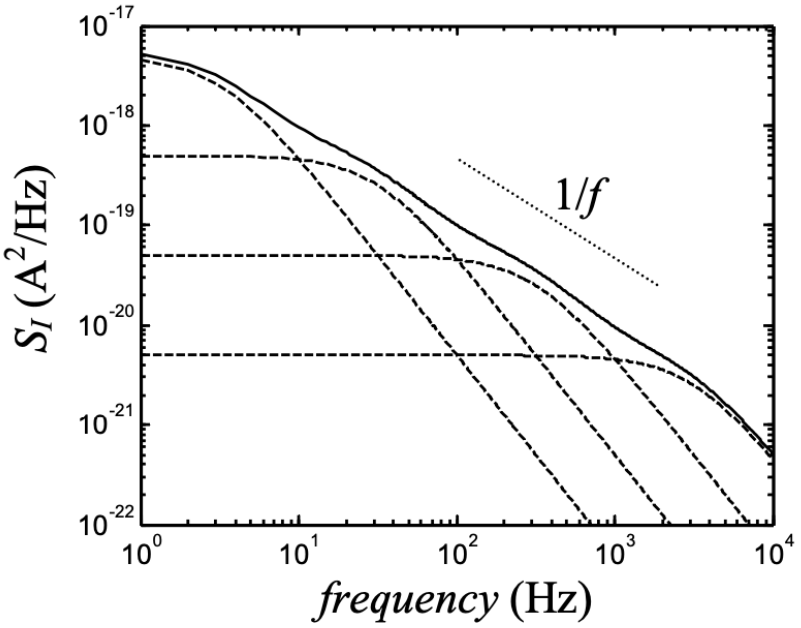

Fig. 2.1 1/f spectrum from a superposition of generation recombination noise [30]

There exist two major models of 1/f noise:

I. Surface Model developed by McWhorter in1957 [31].
II. Hooge developed Bulk Model in 1969 [32].

1/f type of noise is the mobility function which Hooge described with the formula [32]

$$\frac{S_R}{R^2} = \frac{\alpha_H}{fN}; \qquad (6)$$

where f and N represent the frequency and number of charge carriers in the sample respectively, and α_H and S_R represent the Hooge parameter and resistance spectral density. The value of the Hooge parameter can be different for different semiconductor structures and devices [31-32].

1/f^2 noise is a derivative of 1/f noise, and it is found mainly in metal interconnections when integrating circuits. 1/f^2 noise is exhibited for very narrow connections where electromigration is possible due to high current densities. For instance, the electromigration process in aluminum begins at current densities of 200 μA/μm^2, and noise characteristics change from 1/f^2 to 1/f where $\gamma > 2$ [33]. The noise level increases proportionally to the third power of the biasing current [33]. It is very suitable for studies on electromigration because the electromigration mechanism gives rise to these kinds of noise. This type of noise is divergent to burst noise and generation

recombination noise in which the current acts to measure already present conductance noise [32]. An empirical formula for voltage noise spectrum of $1/f^2$ is expressed as

$$s_{\frac{1}{f}^2}(f) = \frac{C.j^{\beta}}{f^{\gamma}.T} \cdot \exp\left(\frac{-E_a}{ch.T}\right); \qquad (7)$$

where: $\beta \geq 3$, $\gamma \geq 2$, which are parameters depending on technology and geometry. C and E_a represent a constant and the activation energy, respectively, and k is Boltzmann's constant.

Burst or RTS noise. Burst noise is another type of low-frequency noise. Burst noise can also be called Random Telegraph Signal noise (RTS), popcorn noise, impulse noise, or bistable noise with a given biasing condition of the device. The magnitude of the device is constant, but the switching time is random [34].

Burst noise is a square wave with random pulse width, as shown in Fig 2.4. Burst noise has two or several different levels, which are displayed as discrete switching events in the time domain.

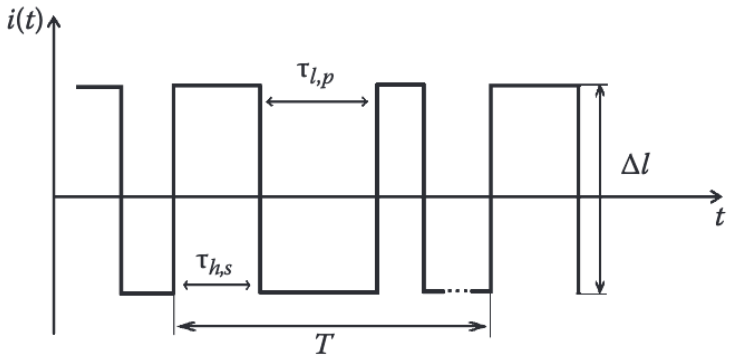

Fig. 2.2 RTS noise or Burst noise [34]

2.8 Importance of Noise Measurement

Noise measurement exhibits an outstanding advantage compared to the accelerated age test of devices. The test conducted measuring the noise in semiconductor devices is far less destructive and more sensitive than dc measurement. In this way, the general quality of the device can be determined, which is a single parameter test to aid in the rejection of low-quality devices and promotes good quality assurance. Excess noise is due to defects that occur in semiconductor devices and the non-ideality of the device [29]. The non-ideality of a device that results in excess noise is due to loss in a capacitor, leakage current, and parasitic resistance [29]. Noise measurement experiments show that device noise level increases as the device degrades or is under stress [34]. Also, suppose the device offers a very high noise level at its primitive stage. In that case, the device is termed to have a short lifetime, and noise is thus a sensitive and non-destructive reliability indicator [29].

Semiconductor devices having a short life can result in failure rate dependency on time which occurs in three stages: infant mortality, steady-state, or wear-out periods. This failure rate includes the growth of dislocations, electrode damage, increased current, high radiated light, and high temperatures. Through noise measurement, we can improve the device's quality, which provides needed information about the device.

Noise spectroscopy deals with the measurement of electrical noise and helps to determine the reliability of electrical devices [29]. Increased electrical noise in an electrical device used in a low-noise system will reduce its quality and sensitivity. Noise measurement is a complex task because the signal to be measured is very weak, and a DC bias current and disturbance from the electronic equipment make it more difficult.

In measuring noise, no stress is applied to the device. However, noise measurement requires very special and sensitive equipment and a quiet environment. Due to low-frequency ranges between 0.1 and 100 kHz, measuring noise takes longer period. In measuring noise, the setup must be built carefully with appropriate shielding, and the use of batteries as power sources is strictly recommended to avoid disturbances injected into the circuits when using the main power source.

2.9 Quality and Reliability of Laser diodes

Device Reliability has been a major problem with semiconductor devices, and although it has been extensively studied, not all aspects of the failure mechanism are fully understood. Nevertheless, much progress has been made since the early days when the device's lifetime lasted for a very short period.

A laser diode lifetime can be described with the well-known bathtub curve, which includes an early failure period, a random failure period, and a wear-out failure period [35-36]. The failure rates in the early failure period are due to assembly and major semiconductor defects, but these weak devices can be screened out with a well-designed burn-in process. The wear-out failure period is characterized by an increasing failure rate at the end of a laser's life. In between early failure period and wear-out failure period is the random failure period, which represents the diode's operation life with a relatively stable failure rate.

In laser diodes, the degradation behavior may be separated into two major processes known as catastrophic and gradual degradation [35]. Catastrophic degradation results from mechanical damage of the mirror facets and leads to partial or complete laser failure. These degradations are characterized by a large threshold current of the laser, accompanied by a decrease in its external quantum efficiency.

Gradual degradation mechanism can be separated into two categories: defect formation in the active region and degradation of the current confinement junction. Research conducted used certain parameters for laser diode quality and its reliability. These parameters include threshold current, aging experiments and measurement at very low biasing currents. Laser diode with low threshold current as it exists in quantum well lasers are very reliable having less defects as compared to lasers with a high threshold current [35].

The gradual degradation is a thermally activated process, for which the lifetime of the laser can be expressed by an Arrhenius equation:

$$\tau = \tau_o e^{\left(\frac{-E_a}{K_B T}\right)}; \qquad (8)$$

where τ_o and E_a represent relaxation time or rate constant factor and activation energy, respectively and T, k_B represents the temperature and Boltzmann constant respectively.

Research conducted on high power and high brightness 900-1000nm single emitter laser diodes grown by MOCVD showed two types of failure modes, with Bulk-defect initiated Catastrophic Optical Damage (BCOD) being the main failure mode [37]. The bulk defect could be an epi-grown defect or a process induced defect during manufacturing process or handling. The second type of failure mode is Catastrophic Optical Damage (COD). This degradation was described by Vanzi et al. [38] in two steps: first a power reduction before any detectable degradation of the optical cavity was observed; this was followed by a very fast degradation. COD starts with light absorbed at facet surface due to carrier-photon recombination at surface states generated by facet cleaving. These states cause local heating at facet and the semiconductor bandgap shrinks with higher temperature, which results in more surface recombination [37]. Rapid temperature increase in this runaway process will eventually cause the semiconductor to melt and cause permanent physical/chemical damage to the laser. COD has been found to be the main failure mode in 808 nm diode lasers when they are working in the wear-out region of the bathtub curve [37].

Scientific research conducted on double buried heterostructure lasers with layers above and below the active region having a larger bandgap than that of the active region makes it possible to confine carriers [39]. Also, the materials above and below the active region having a higher index of refraction than the active region produces a wave guide effect that makes it possible to confine light thus making a double buried heterostructure laser with such properties to keep a high concentration of both charge carriers and light in the active region improving the efficiency and its reliability [39]. Buried heterostructure laser diodes are characterized by their low threshold current and high efficiency. This can be achieved by strict injection current and optical field confinement in the active region by current blocking layers. But with the addition of etching processes and the regrowth of more current blocking layers, introduces defects between the active region and the current blocking layers, which leads to a worst laser diode operation and quick degradation resulting in laser diode having a short life span [40].

Laser diodes have unsolved quality and reliability issues owing to various defects which exist in them, and low frequency noise measurement is a good method to investigate laser diodes.

3 Noise Measurement and Calculation Methods

In this research work the following measurements of laser diodes are performed:

1 Current-voltage characteristics;

2 Light output power dependency;

3 Low-frequency noise measurement:

   a) Optical noise;

   b) Electrical noise;

   c) Cross-correlation factor between optical and electrical noise;

4 Temperature characteristics.

Measurements were carried out at room temperature and in temperature range from 88 K to 300 K. Low-frequency noise characteristics were investigated in frequency range from 10 Hz to 22 kHz and at current ranges from 0.1 mA to 140 mA. These measurements were performed with the sample shielded with a laboratory shield (Faraday cage) which helps avoid parasitic electromagnetic radiation.

3.1 Measurement of Current-Voltage Characteristic

Measurement of current-voltage characteristics is essential for calculating the current flowing through the device at a specific voltage. In this work, current-voltage characteristic of the investigated laser diode was measured using the Keysight B1500a Agilent technology semiconductor device parameter analyzer. The operation current of the laser diodes is up to 100 mA and the operation voltage is up to 4 V.

It is observed that excess noise results from the non-ideal components of the flowing current of the semiconductor diode and is caused by the leakage current, parasitic resistance, and other defects [29]. There is a need to determine a non-ideality factor of the current voltage characteristics of semiconductor diode. For current-voltage characteristics, calculation of the factor of the non-ideality (η) is performed, which describes the deviation of the laser diode from the ideal behavior. Value of the non-ideality factor typically varies from 1 to 2 (for an ideal diode η = 1) [41]. The non-ideality factor is derived from the ideal diode equation, which is given by the equation below:

$$I = I_O(e^{\frac{qV}{nkT}} - 1); \qquad (9)$$

$$\eta = \frac{q}{kvT} \cdot \frac{\Delta V}{\Delta log I};$$

$$\frac{q}{kvT} = 0.01846;$$

where I, I_o, V represent the current of the diode, dark saturation current, and voltage of the semiconductor diode, respectively, and q, η, T, k represents the charge of an electron, the non-ideality factor, temperature, and Boltzmann's constant, respectively.

From the ideal diode equation (9) the non-ideality factor can be calculated as:

$$\eta = 0.01846 \cdot \frac{\Delta v}{\Delta log I}. \qquad (10)$$

3.2 Light Output Power Dependency

Measurement of light output power represents the output light intensity versus the driving current applied to the laser. It also represents the amount of light from the laser diode detected by the photodiode. Light output power is used to determine the lasers operating point and threshold current which is strongly affected by temperature.

In this work, light output power dependency is measured in the same setup as noise was measured. A difference is that a voltmeter is used to measure the voltage of the photodiode which represents light intensity. In conducting the experiment setup should be shielded in the Faradays cage and against all visible light sources for better results.

3.3 Low-Frequency Noise Measurement

In any optoelectronic device investigation, it is very relevant to know the optical noise characteristics, which are the output power fluctuations, electrical noise, which is the diode terminal voltage fluctuations and the correlation between optical and electrical fluctuations. In this work, characteristics of low frequency electrical and optical fluctuations and cross-correlation between optical and electrical noise signals were investigated for laser diodes.

The measurement setup designed to measure low-frequency noise is shown in Fig. 3.1. The electrical noise of laser is measured by registering fluctuations of its voltage, while optical noise is measured by registering voltage fluctuations of photodiode illuminated by the laser under investigation.

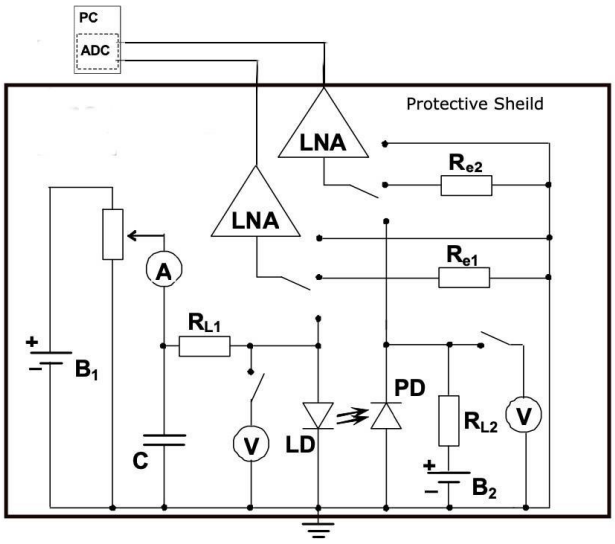

Fig. 3.1 Circuit for measuring optical and electrical noise.

A laser diode emits light, and the photodiode detects its power fluctuations. An external 12 V battery is used to forward bias the laser diode, and a photodiode is reversed biased with another external battery of 9 V. External batteries are used to avoid interference from main power lines. The current of the laser was varying with an adjustable resistor and measured with an amperemeter. The entire setup needs to be shielded because noise is a weak signal. This prevents interference from external radio transmitters and other light sources. Only the amplified noise signal is routed out of the shield. The noise was measured within current ranges between 0.1mA and 110mA.

Since the light is emitted out of the facet laterally, there must be a clear optical path for the light as it exits the laser. To ensure the most stable operating environment and provide outstanding protection for the laser diode when measuring its noise, it should be mounted on a copper radiator with low thermal resistivity. This is because semiconductor laser structure dimensions are very small, leading to large current density and Joule heating.

In conducting noise measurement, optical and electrical noise signals should be measured simultaneously, making it possible to calculate the correlation between two noise signals. Also, it is first necessary to measure the system's own noise, and this can be performed by short-cutting of low noise amplifiers input. Fig. 3.2 shows the system's own noise.

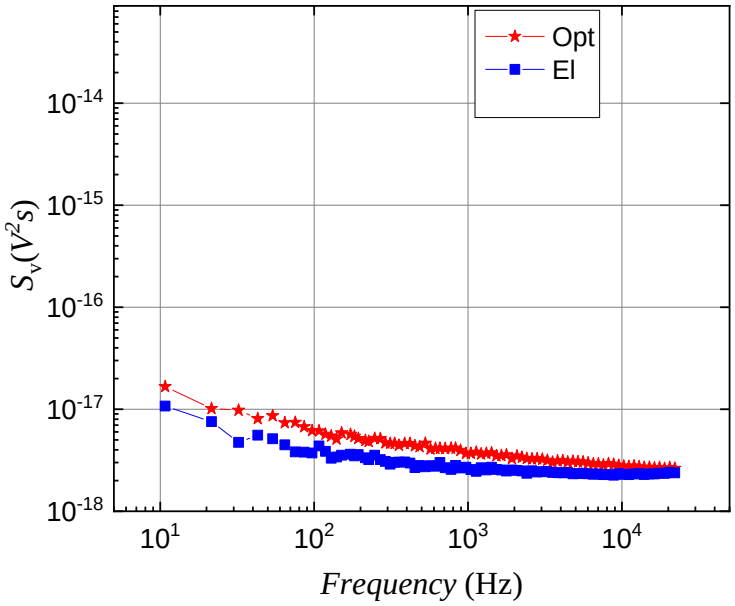

Fig. 3.2 Noise spectral density of the measuring system

Electrical noise signal, once amplified, is passed to an oscilloscope for monitoring of the signals which is measured. Since noise is termed a very weak signal, the measurement system must have a good gain factor in which the gain factor could be used to detect and measure noise signal. The gain factor used in this noise measurement is in decibels (dB). The noise signal is then digitized and passed on to the computer using a soundboard as an analog-digital converter. The window of software used to measure noise is shown in Fig. 3.3.

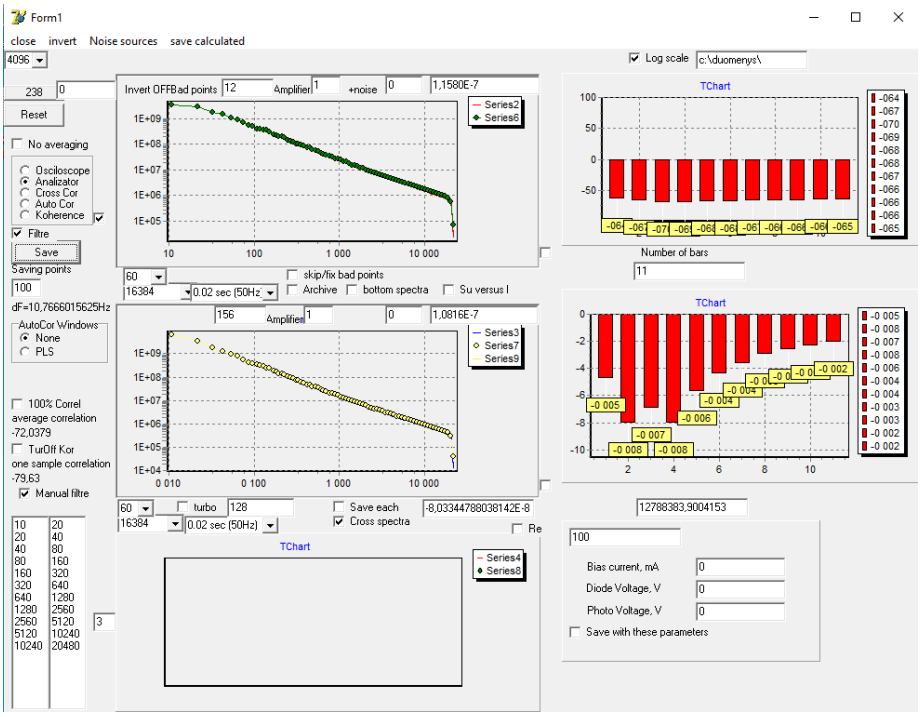

Fig. 3.3 Window of the noise measurement software.

Measurement signal was controlled by the visual observation in the oscilloscope and on the software window. The software can display signals which are measured in time and frequency domains. It is required to use a signal in the time domain. When a suitable and clear signal is obtained on the software and oscilloscope, the selected gain is used, which shows a correct gain factor and the system signal is switched to the frequency domain, and noise signal is measured. The noise spectral density of voltage fluctuations is estimated using the Cooley-Turkey Fast Fourier Transform-based spectrum analyzer program [42].

The average noise spectrum is obtained, and the noise spectral density is calculated by comparing it with the thermal noise of the reference resistor. Noise spectral density of optical noise is calculated with the following formula:

$$S_{\mathrm{vopt}}(V^2\mathrm{s}) = \frac{k_1 S_{\mathrm{opt}} - k_2 S_{\mathrm{Short}}}{k_3 S_{\mathrm{resistance}} - k_2 S_{\mathrm{short}}} \cdot 4kTR; \qquad (11)$$

where $k_1, k_2,$ *and* k_3 represent amplification factors for the input optical signal, short and resistance signals respectively, S_{opt}, $S_{\mathrm{Resistance}}$, S_{short} represent the noise of optical signal of the device under investigation, noise of the reference resistance and noise of the measuring system respectively and k, T, R represents Boltzmann's constant temperature and resistance.

Noise spectral density of electrical noise is calculated with equation (12). The spectral density is evaluated also by comparing it with the thermal noise of the reference resistor *R*.

$$S_{\mathrm{vel}}(V^2\mathrm{s}) = \frac{k_1 S_{\mathrm{el}} - k_2 S_{\mathrm{Short}}}{k_3 S_{\mathrm{resistance}} - k_2 S_{\mathrm{short}}} \cdot 4kTR; \qquad (12)$$

where $k_1, k_2, \; and \; k_3$ represent amplification factors for the electrical signal short and resistance signals respectively, S_{el}, $S_{\mathrm{Resistance}}$, S_{short} represents the noise of electrical signal of the device under investigation, noise of the reference resistance and noise of the measuring system respectively and k, T, R represents Boltzmann's constant temperature and resistance.

Cross-correlation factor shows how strongly electrical and optical noise spectral densities are related. Cross-correlation measurement between electrical and optical noise helps to identify whether the low-frequency fluctuations originate from the active layer of the laser sample or its peripheral components [43]. The noise software calculates the cross-correlation coefficient for every octave. Frequency octaves span through all measured frequency ranges which are inputted into the software. (10-20 Hz), (20-40 Hz), (80-160 Hz), (160-320 Hz), (320-640 Hz), (640-1280 Hz), (1280-2560 Hz), (2560-5120 Hz), (5120-10240 Hz), (10240-20480 Hz). Cross-correlation, which was simultaneously calculated, is given in the equation (13):

$$k = \frac{\frac{1}{N}\overline{\sum_{i=1}^{N} V_i^{\mathrm{el}} V_i^{\mathrm{opt}}}}{\sqrt{\frac{1}{N}\overline{\sum_{i=1}^{N} (V_i^{\mathrm{el}})^2}}\sqrt{\frac{1}{N}\overline{\sum_{i=1}^{N} (V_i^{\mathrm{opt}})^2}}} \cdot 100\%; \qquad (13)$$

where $\sqrt{\frac{1}{N}\overline{\sum_{i=1}^{N}(V_i^{\mathrm{el}})^2}}$ and $\sqrt{\frac{1}{N}\overline{\sum_{i=1}^{N}(V_i^{\mathrm{opt}})^2}}$ are the root mean square values of signals of electrical and optical noise, which corresponds to the fluctuation voltages at the terminal

3.4 Measurement of Temperature Characteristic

For temperature characteristics measurement, the investigated laser is mounted on a radiator and placed in a thermo-isolated chamber for stabilization of sample temperature. The thermo-isolated chamber is sealed and mounted in a Faraday cage. Liquid nitrogen is poured on the surface of the thermo-isolated chamber which is used for cooling the laser. The laser is cooled to a very low temperature and measurements are taken in the range from 88 K to 300 K. Temperature is controlled by a thermo resistor located in the thermo-isolated chamber.

3.5 Modelling of Noise Spectra

In this research, experimental noise spectra measured at different temperatures were analyzed. Low-frequency electrical voltage noise spectra of laser diode can be represented as a sum of independent components of 1/*f*, $1/f^{\alpha}$, Lorentzian type spectrum due to generation and recombination processes in various defects and impurities with different relaxation times and white noise spectrum for shot noise [33-34]. The presented sum is shown in equation (14):

$$S_{\text{el sum}}(f) = \frac{A_{\text{el } 1/f}}{f} + \frac{A_{\text{el } 1/f^{\alpha}}}{f^{\alpha}} + \frac{A_{\text{el gr } \tau}}{1+(2\pi f\tau)^2} + S_{\text{el shot}}\ ; \quad (14)$$

where $A_{\text{el } 1/f}$ defines intensity of the noise component of the 1/*f* noise, $A_{\text{el } 1/f^{\alpha}}$ defines intensity of the noise component of $1/f^{\alpha}$, $A_{\text{el gr } \tau}$ defines intensity of the noise component of generation and recombination noise and $S_{\text{el shot}}$ defines the shot noise.

To identify traps, experimental noise measurement is fitted to extract the characteristic slope of $1/f^{\alpha}$ type component (α) and the relaxation time of each trap contributing to GR noise (τ). The generation-recombination noise is characterized by a Lorentzian spectrum with a time constant τ. Two processes of generation and recombination are used for the approximation. Experimental approximation is made with equation (14) with no shot noise component since the spectrum consisted mainly of 1/*f*, $1/f^{\alpha}$ and two GR noise components. The relaxation time $\tau = 1/2\pi f$ is a better-defined quantity, but it still requires some model for its interpretation [27]. In most semiconductor devices, it is thermally activated, what is described by the Arrhenius formula used in the case of thermally activated GR centers. The Arrhenius formula is shown in equation (15) is used to evaluate the activation energy of each GR center:

$$\tau = \tau_o e^{\left(\frac{-E_a}{K_B T}\right)}; \quad (15)$$

where τ_o and E_a represent relaxation time or rate constant factor and activation energy, respectively and T, k_B represents the temperature and Boltzmann constant respectively.

3.6 Investigated Devices

Investigated devices involve laser diode with quantum well between rectangular and parabolic barriers. The investigated laser diode were grown using two SVT-A and Veeco GENxplor R&D molecular beam epitaxy (MBE) reactors. Device structures were based on GaAs and GaAsBi compounds in QWs. Laser diodes have been grown under standard conditions: 650°C temperature and arsenic overpressure. Table 3.1 summarizes the investigated device.

Table 3.1 Investigated devices.

Device	QW Material	Shape/Structure	Fabrication method
PQW	GaAs	Parabolic Quantum Well (PQW)	MBE
RQW1	GaAs	Rectangular Quantum Well (RQW)	MBE
RQW2	GaAs	Rectangular Quantum Well (RQW)	MBE
RQW-Bi	GaAsBi	Rectangular Quantum Well (RQW)	MBE

4 Results and Discussion

This chapter presents results representing a comprehensive investigation of current-voltage characteristics, light output power dependency, low-frequency noise characteristics, cross correlation factor and temperature characteristics of the investigated laser diodes.

4.1 Operating Characteristics of Investigated Laser Diodes

The operating characteristics of the investigated laser diodes represent the current-voltage characteristics and the light output power dependency on injection current (Fig 4.1). The current-voltage characteristics of the investigated laser diodes were measured not only in the operating range of the diode but also at a very low current range between 1 mA to 100 mA and at voltages between 0 V and 4 V. Current voltage characteristics for laser types with rectangular and parabolic quantum wells were very similar for *pn* diodes: current-voltage characteristics of *pn* diodes is exponential, with the non-ideality factor between 1 and 2. From our experiment, the non-ideality factor for RQW1, RQW2, PQW and that of GaAsBi is 1.01, 1.02,1.12 and 1.86 respectively, indicating that current is comprised of diffusion and generation and recombination current components. Current voltage characteristics of GaAsBi laser diode showed some variations from rectangular and parabolic samples due to reduction in bandgap of the laser diode sample this is because of the presence of bismuth in the laser structure.

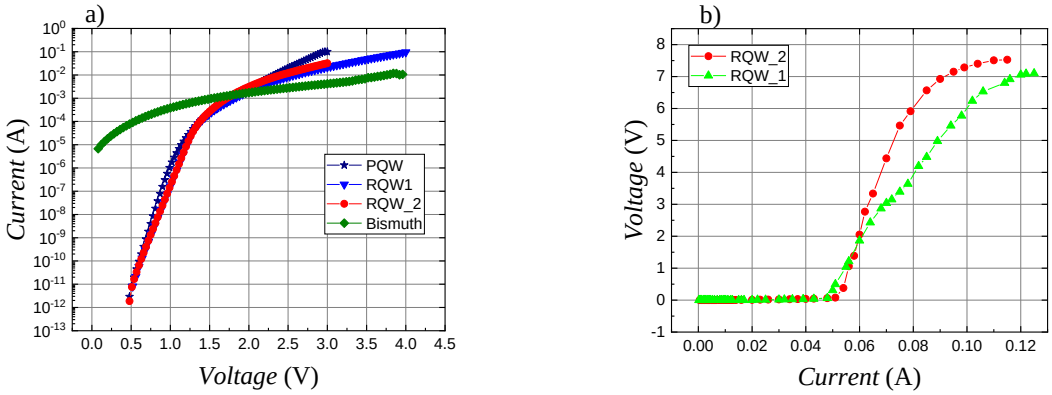

Fig. 4.1. Operating characteristics of investigated laser diodes at room temperature: a) current-voltage characteristics, b) light output power.

Light output power of investigated laser diodes characterizes their emission properties. Light output power of RQW1 and RQW2 lasers is shown in Fig 4.1b. which increases linearly above threshold up to some current where saturation starts. There is a sharp increase of incline at a current

of 50 mA and 52mA for RQW1 and RQW2, respectively- this current is threshold current. The threshold current of such laser diodes varies from 50 mA to 120mA [44]. In light output power characteristics, the slope of the curve above the threshold is larger than slope observed below the threshold. Light emission appearing below the threshold is mainly spontaneous emission whereas above threshold is stimulated emission. A more noticeable saturation of the light output characteristics is observed for RQW2 laser. At current between 60 mA and 80 mA some changes in incline of the light output power characteristics for RQW1 are observed what indicates reduction in efficiency of laser.

4.2 Low-Frequency Noise Characteristics at Room Temperature

Low-frequency optical and electrical noise measurement was carried out at room temperature for RQW1 and RQW2 laser diodes in current ranges from 10 mA- 100 mA and at a frequency of 10 Hz to 20 kHz; electrical noise measurement was also carried out for PQW and GaAsBi lasers. Results obtained for optical and electrical noise characteristics for investigated lasers are presented in Figs. 4.2-4.8.

4.2.1 GaAs Based Rectangular Quantum Well Laser Diodes

Optical noise spectra of RQW1 laser diode at current range 10 mA- 96 mA and RQW2 at current ranges 10 mA- 80 mA are shown in Figs 4.2a and 4.2b. Optical noise spectra at room temperature are $1/f$ type. Optical noise intensity increases with increasing forward current: optical spectra of RQW1 at the threshold current (> 50 mA) and optical spectra of RQW2 at the threshold current (> 52 mA) showed a sharp increase in noise spectra density. Optical noise intensity dependency on current (Fig. 4.4a) of the RQW1 and RQW2 laser diodes has a sharp peak at the threshold current: 50mA and 52mA, respectively. This is as a result of the change in operation mode from the light-emitting diode to the laser diode operation mode: at the threshold current light output power of laser diode becomes much more intensive and therefore its fluctuations become larger. Optical noise intensity is larger for RQW2 than RQW1.

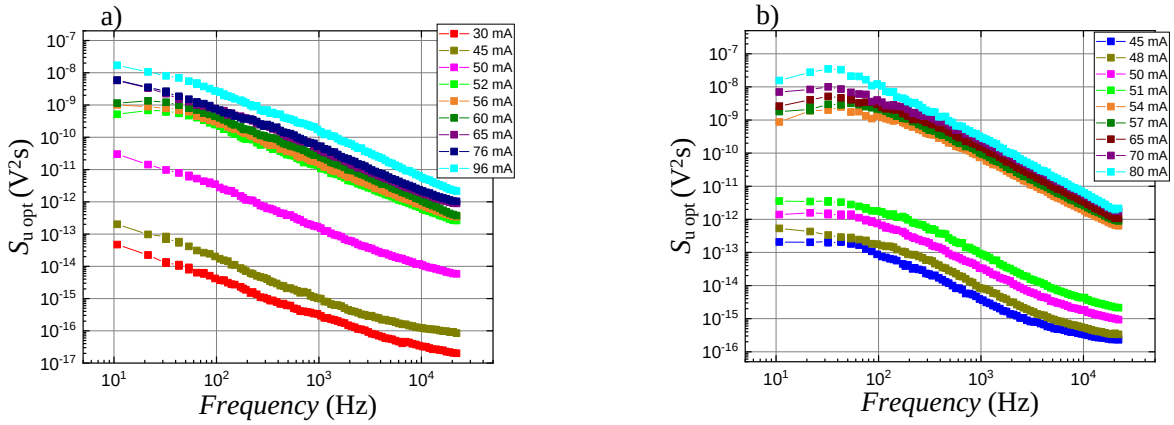

Fig. 4.2. Optical noise spectra at room temperature at current ranges 30 mA-100 mA: a) RQW1, b) RQW2.

Electrical noise spectra of RQW1 and RQW2 lasers below and above threshold current are shown in Fig. 4.3. The electrical noise spectra of both rectangular quantum well lasers are characterized by 1/*f* and Lorentzian type spectrum components. The source of 1/*f* type noise in semiconductor devices is generally caused by superposition of the generation and recombination (GR) charge carrier. These GR centers are formed by different defects, dislocations, and imperfections in the device structure. The noise intensity increases with increasing forward current (Fig 4.4). At current ranges between 60 ma – 96 ma, 1/*f* noise approaches white noise at high frequency (above 10kHz) for RQW1 laser sample: this is seen by a slight deviation in linearity of the spectrum (Fig 4.3c). In Fig 4.3d for RQW2 laser, it can be seen that noise spectral density is very large at current range 70 mA- 90 mA. This large electrical and optical noise intensity is related to noticeable saturation of light output power (Fig 4.1b).

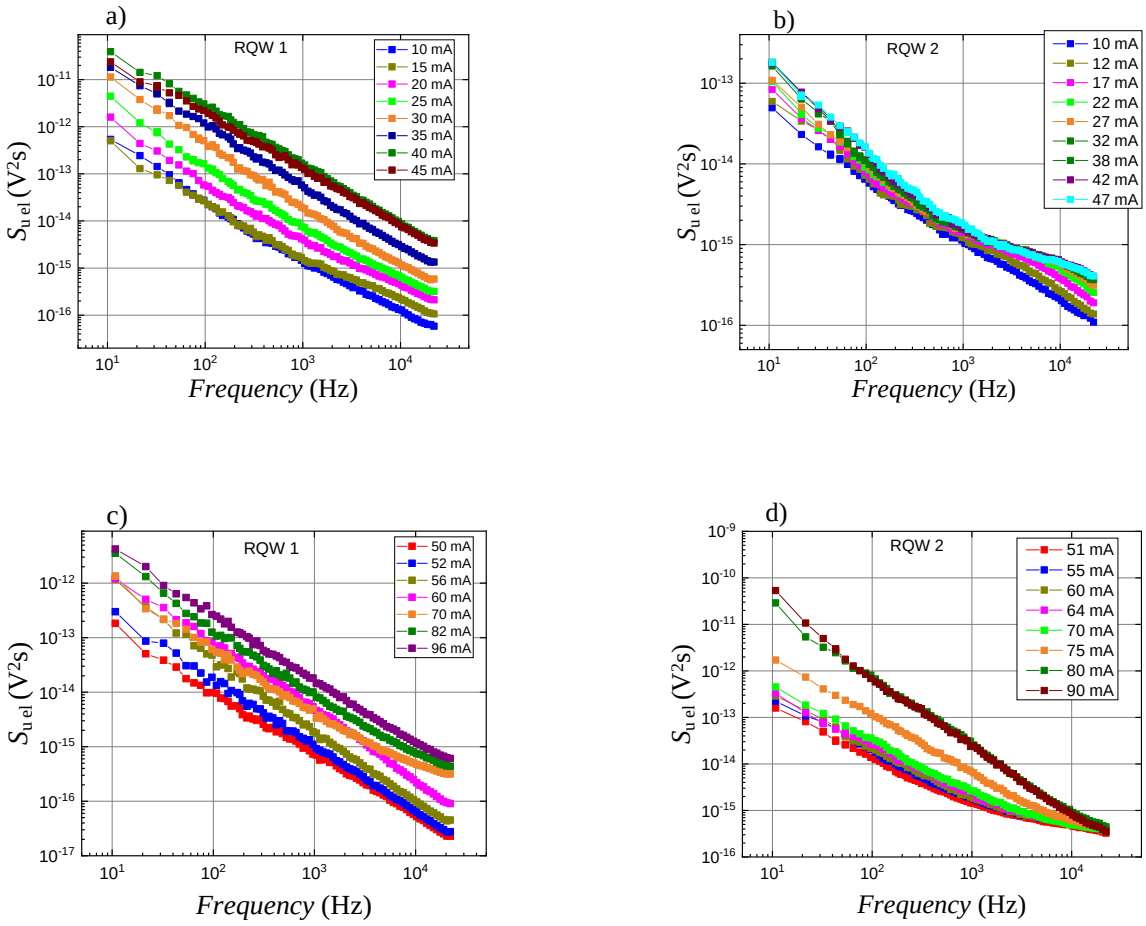

Fig. 4.3. Electrical noise spectra at room temperature at current 10 mA-100 mA: a) and c) RQW_1, b) and d) RQW_2.

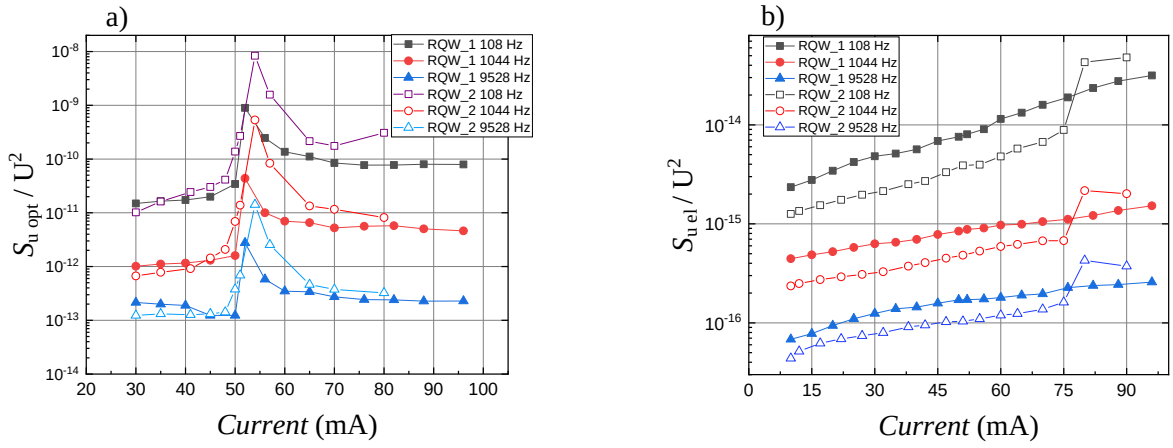

Fig. 4.4. Noise spectral density dependencies on forward current at room temperature for RQW_1 and RQW_2 lasers: a) optical fluctuations, b) electrical fluctuations

4.2.2 GaAsBi Based Rectangular Quantum Well Laser Diode

Results obtained for electrical noise characteristics of GaAsBi based laser diode are presented in Figs. 4.5-4.6.

1/*f* type spectra are observed in low-frequency noise characteristics of GaAsBi laser diode. Electrical noise spectrum shows a clear 1/*f* type noise component over the measured frequency range over all measured currents. Noise intensity is very large compared to RQW1 and RQW2 lasers what indicates larger defectivity of this type of lasers.

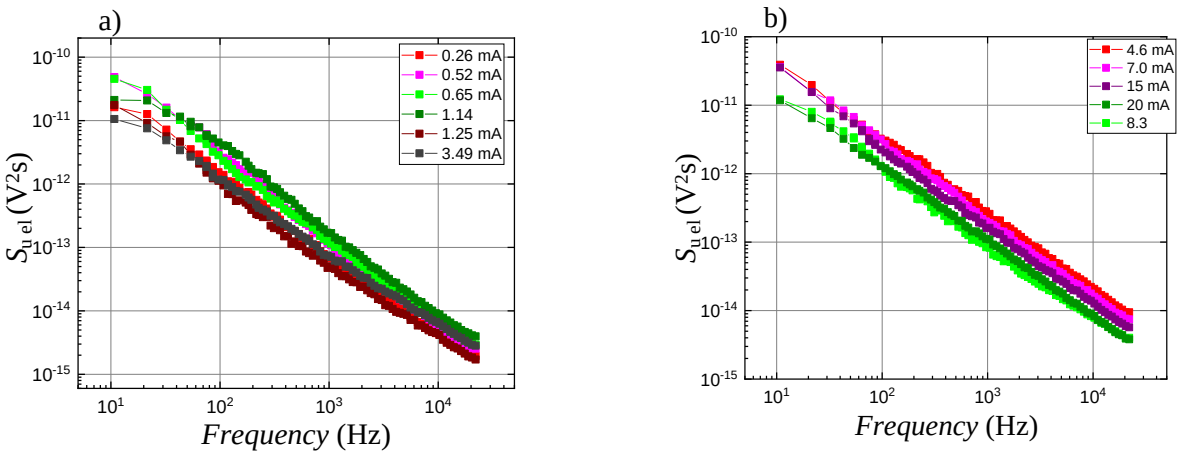

Fig. 4.5. Electrical noise spectral density dependencies on frequency at room temperature for GaAsBi laser diode: a) small currents, b) larger currents.

Electrical noise spectral density dependence on current in Fig 4.6 shows fluctuation in noise spectral density as we increase forward current. Noise spectral density decreases or increases in a small order of magnitude as current is varying. The source of 1/*f* type noise in semiconductor devices is generally caused by the superposition of processes of charge carriers generation and recombination (GR). These GR centers are formed by different defects, dislocations, and imperfections in the device structure.

Larger defectivity of Bismuth laser causes larger 1/*f* noise intensity compared to RQW1 and RQW2, and at small current, current follows through defects formed channels what causes larger noise, and noise level decreases with current increases as current flows through all cross sections. While RQW1 and RQW2 laser are less defective, noise intensity is low and proportional to forward current.

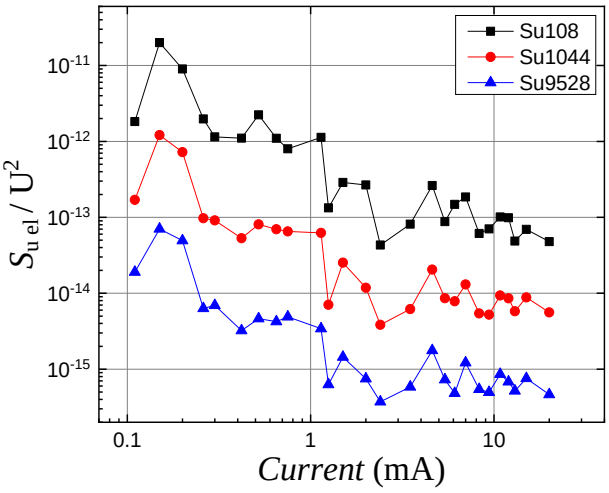

Fig. 4.6 Noise spectral density dependency on forward current at room temperature for GaAsBi laser diode.

4.2.3 GaAs Based Parabolic Quantum Wells Laser Diode

Electrical noise measurement results obtained for PQW laser diode are present in Figs 4.7 and 4.8. Electrical noise spectral density of PQW laser diode at currents between 5 mA- 75 mA is characterized by the Lorentzian type of spectrum, which is characteristic for generation recombination process, and 1/*f* noise components. The 1/*f* noise component up to 0.1 kHz and an intensive component of generation and recombination noise up to about 10kHz is seen at currents between (5 mA-10 mA). 1/*f* noise increases, and generation and recombination noise decrease at currents between (28 mA-75 mA). Current-voltage characteristics of this sample shows almost only diffusion current and very small influence of generation and recombination processes to current flow. This shows that low frequency noise measurement is more sensitive than the current-voltage characteristics to the presence of such defects.

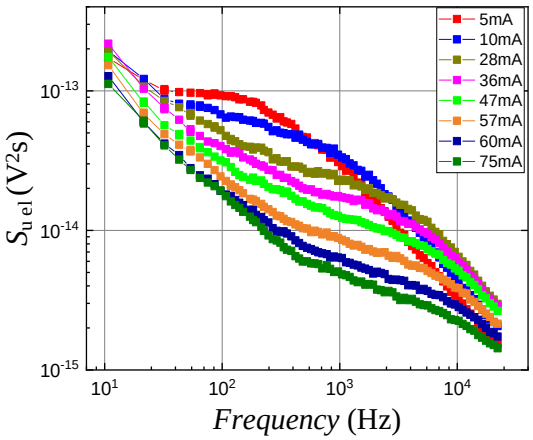

Fig 4.7 Electrical Noise Spectra of PQW laser diode at room temperature at forward current 5 mA-75mA.

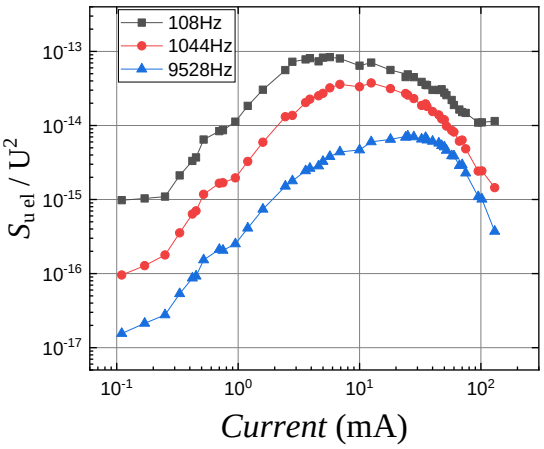

Fig 4.8 Electrical noise spectral density dependency on current at room temperature for PQW laser diode.

Electrical noise spectral density dependencies on current are shown in Fig 4.8. Noise intensity increases as the current increases at various frequencies which can also be observed in Fig. 4.7.

Comparing all four investigated laser diodes: GaAs based lasers with rectangular and parabolic and GaAsBi based laser diode, GaAsBi laser diode showed a very high electrical noise intensity which is caused by larger defects in this type of laser. This defectivity of GaAsBi based structure can be a result of surface segregation and formation of clusters when bismuth is grown over very high temperature [3].

Noise characteristics of lasers with rectangular and parabolic QWs show that quality of the investigated NIR laser diode does not depend on the profile or shape of quantum wells.

4.3 Cross-Correlation between Optical and Electrical Fluctuations of Laser Diode.

Averaged cross-correlation factor between optical and electrical fluctuations of GaAs RQW laser diode in frequency range 10 Hz to 20 kHz and in every frequency octave with central frequencies, fc (Hz): 15, 30, 60, 120, 240, 480, 960, 1920, 3840, 7680, 15360 are presented in Figs. 4.9 and 4.10. Considering that light emission is from the active region of the laser, the correlated electrical and optical low-frequency $1/f$ type fluctuations can be related to defects in the active region or defects at the active region interface. High positive cross-correlation factor between optical and electrical $1/f$ noise indicates high density of defects and imperfections in the active region. Active region defects and imperfections not only change the noise level in the device

but also increase its non-radiative recombination process and decrease laser efficiency. Cross-correlation dependency on the frequency for RQW1 and RQW2 is shown in Figs. 4.9a and 4.9b, respectively. Measured cross-correlation factor increases with increasing forward current due to the rise in light output power (Fig 4.10). The result shows that dominating noise components above threshold at low frequency are highly correlated.

Cross-correlation factor between 1/*f* optical and electrical noise component for both investigated samples is not 100%, what shows that not all fluctuations are completely correlated. This means that not all 1/*f* electrical fluctuations generate optical fluctuations resulting in noise origin not only occurring from the active region of the investigated lasers.

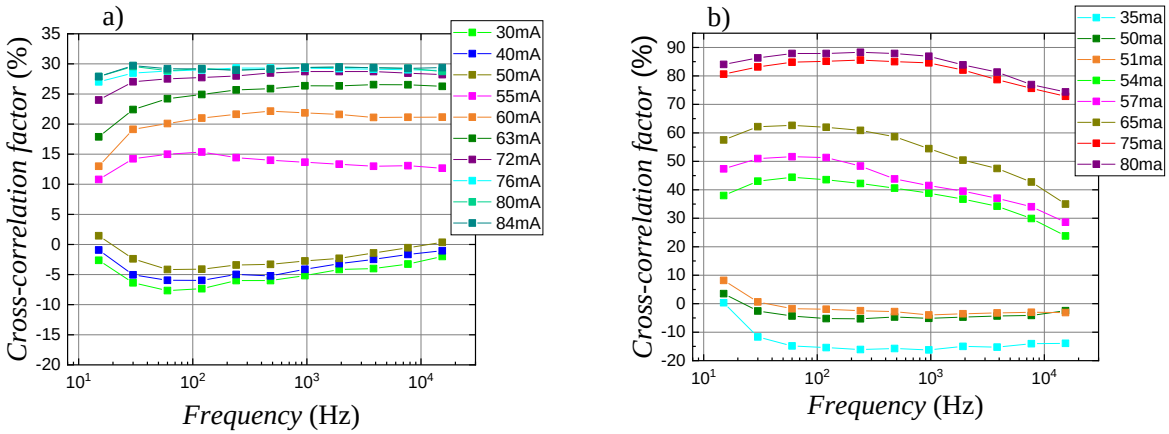

Fig 4.9. Cross-correlation factor dependency on frequency: a) RQW1, b) RQW2.

Cross-correlation factor dependency on current (Fig 4.10) shows a negative cross correlation factor at currents below the threshold current (50 mA) for both RQW1 and RQW2 laser diodes. At currents above the threshold current, larger positive cross correlation between optical and electrical fluctuations is seen for both investigated laser diodes being larger for RQW2 than for RQW1. This endorses that RQW2 sample has lower quality (higher defectivity) than RQW1 which was also noticed from light output power and electrical noise characteristics. Concerning the investigated lasers operation above threshold, cross-correlation factor decreases with current due to better fulfilled conditions of laser generation.

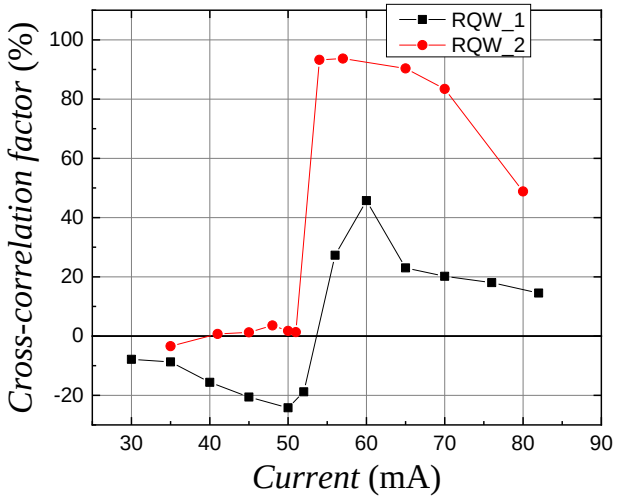

Fig 4.10. Cross-correlation factor dependency on current at frequency range 10 Hz – 20 kHz

4.4 Electrical Noise Characteristics at Different Temperatures

Theoretical and experimental temperature characteristics of electrical fluctuations of PQW laser diode are measured and analyzed. Temperature characteristics at a fixed 10 mA current and temperature characteristics at various temperatures at different currents are presented in Fig. 4.11-4.13.

The spectra observed in Figs 4.11a and 4.11b consists of two components of Lorentzian type spectrum, which are due to more intensive generations and recombination processes (comparing to other generation and recombination processes whose superimposition results in 1/*f* noise spectrum). The slope of 1/*f* and Lorentzian bump are similar over all measured temperature range (88 K-300 K). It can also be seen that the noise spectral density does not depend on the temperature at lower temperature but starts to decrease with temperature above 150 K (Fig. 4.12).

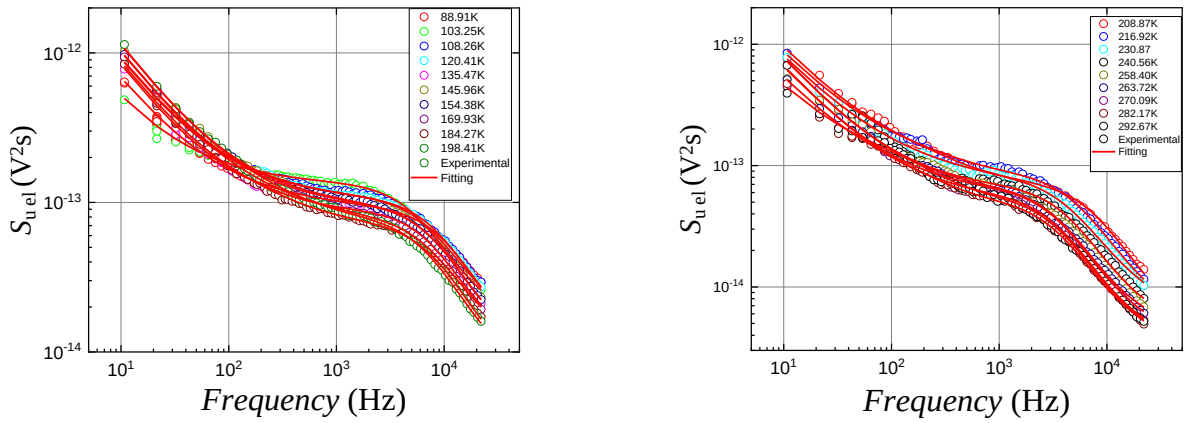

Fig 4.11. Electrical noise spectral density dependencies on frequency at 10mA current at different temperature ranges: a) 88.91 K-198.41 K, b) 280 K-293 K (symbols represent experimental date, solid lines - for modeling results).

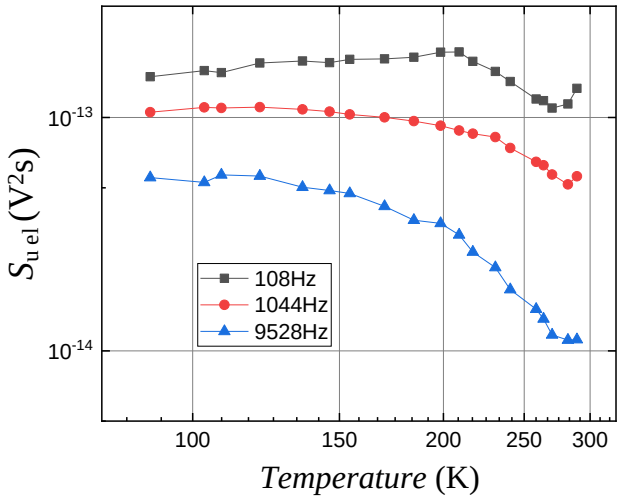

Fig. 4.12 Electrical noise spectral density dependencies on temperature.

Noise spectral density dependence on frequency at some specific temperatures between (175 K-225 K) at different currents varying between 4 mA-20 mA was also measured and is shown in Fig 4.13. At the presented temperatures, presence of 1/*f* and clear Lorentzian type spectrum component is observed. Intensity of 1/*f* noise increases with current increase and thus shifts to higher frequencies, while Lorentzian type component decreases in this case.

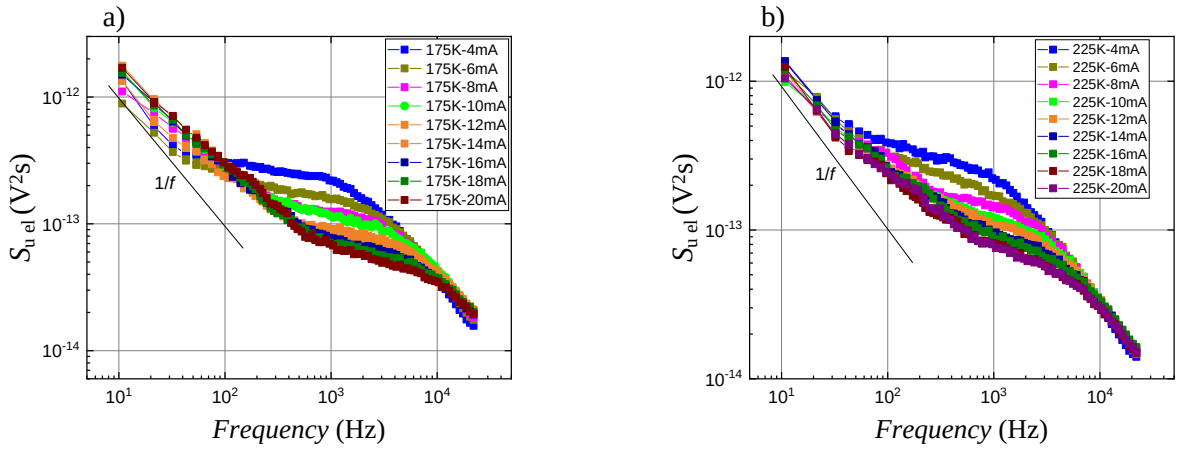

Fig 4.13 Electrical noise spectral density dependencies on frequency at fixed temperature and current ranged 4 mA-20 mA: a) T=175 K, b) T= 225K.

4.5 Modelling of Noise Spectra

To identify traps or trapping centers, experimental noise spectra presented in Fig 4.13 were modelled and data fitted to extract the characteristic slope (α) of the $1/f^{\alpha}$ type spectrum and the relaxation time (τ) of each trap contributing to the noise. For this purpose, noise spectra were approximated and modeled by equation (16).

$$S_{\mathrm{el\,sum}}(f) = \frac{A_{\mathrm{el}\,1/f}}{f} + \frac{A_{\mathrm{el}\,1/f^{\alpha}}}{f^{\alpha}} + \frac{A_{\mathrm{el\,gr1}}\tau_1}{1+(2\pi f\tau_1)^2} + \frac{A_{\mathrm{el\,gr2}}\tau_2}{1+(2\pi f\tau_2)^2}\,; \qquad (16)$$

This equation is similar to equation (14). It was found that obtained experimental data are well approximated by the sum of the $1/f$ noise component, $1/f^{\alpha}$ noise component and two GR noise components (shot noise is too small to count it). The generation and recombination noise is characterized by Lorentzian spectrum with a time constant τ. Spectra are analyzed for various temperature ranges between 175 K to 225 K at different current ranges between 4 mA - 20 mA. The obtained results are presented in Fig 4.14.

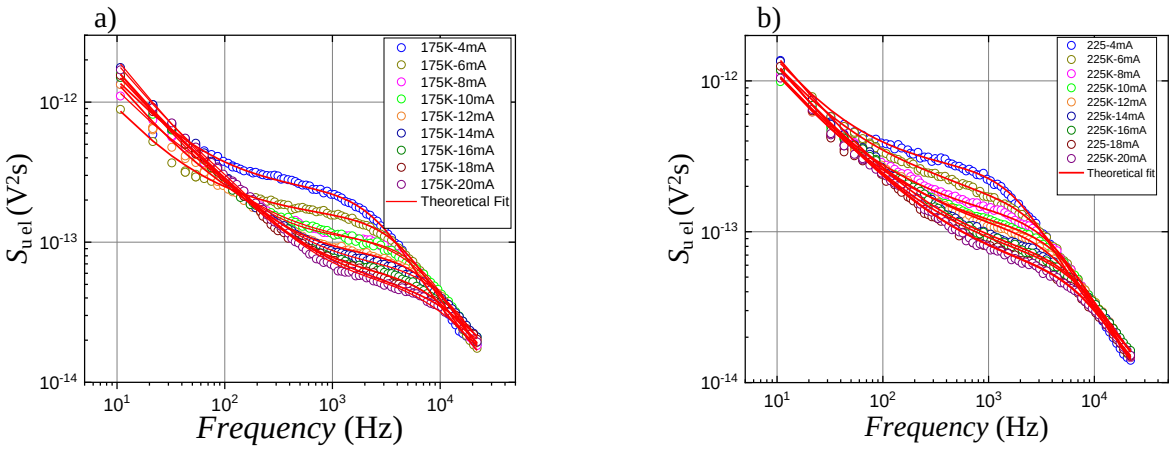

Fig. 4.14. Modelled noise spectral density dependencies on frequency at fixed temperature and in current ranges 4 mA-20 mA: a) *T*= 175 K, b) *T*= 225K (symbols represent experimental date, solid lines - for modeling results).

The two GR centers GR1 and GR2 contributing to the low-frequency noise are extracted from each different spectrum. The characteristic times and the activation energy of trapping centers are evaluated for GR 1 and GR 2 using the Arrhenius plot, which is shown in Fig. 4.15.

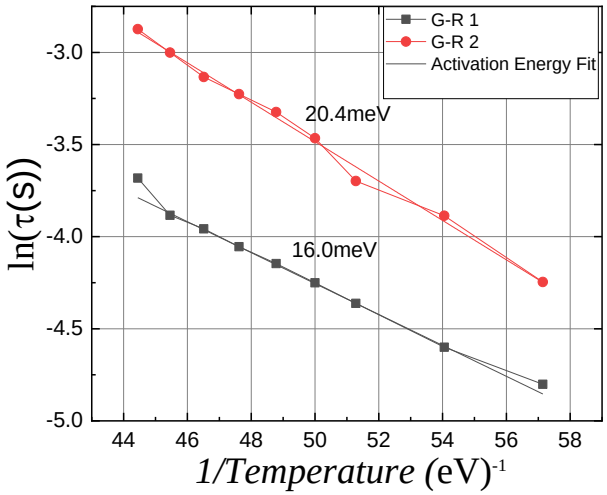

Fig. 4.15 Arrhenius plot of relaxation time as a function on inverse temperature.

The origin of many thermally driven processes may be identified by measuring their activation energy. Generation and recombination noise can be used as a tool to characterize traps in semiconductors. These traps in the investigated laser diode are responsible for capture and emission of carriers and are described by their activation energy. Lorentzian spectrum

characteristic relaxation time constant τ depends exponentially on temperature. The two GR centers GR1 and GR2, contributing to the low-frequency noise are extracted from each spectrum. Figure 4.15 illustrates the Arrhenius plots for trapping centers. The activation energies are determined by finding the slope of the straight line with activation energy of GR1 and GR2 to be 16 meV and 20.4 meV respectively.

5 Conclusions

1. Current-voltage characteristics of the investigated laser diodes have non-ideality factor between 1 and 2 which is close to the ideal behavior of diodes: the main current components are diffusion and generation and recombination. Low frequency noise spectra of the investigated laser diodes show $1/f$ and Lorentzian type spectrum components, which are caused by generation and recombination of charge carriers.
2. Electrical noise voltage spectral density of rectangular GaAsBi QW based laser diode is about two orders of magnitude larger than rectangular and parabolic GaAs QW based laser diode, what shows that presence of Bismuth increases defectivity of the laser structure.
3. Low-frequency noise characteristics do not depend on the quantum well shape or profile (rectangular or parabolic) for the investigated laser diodes.
4. Faster saturation of light output power, increase in electrical and optical noise intensity, at threshold and decrease in cross-correlation at current ranges 70 mA- 80 mA in RQW2 laser diode indicate larger current leakage out of the active region in this structure.
5. Modelling of electrical noise spectra of parabolic quantum well laser diode analyzed at temperature ranges 88 K – 300 K shows that noise spectra mainly comprise from thermal, $1/f$, $1/f^{\alpha}$ and two Lorentzian type components with α varying from 0.15 to 1.55 and activation energies of the observed two generation and recombination processes: 16.0 meV and 20.4 meV.

LOW-FREQUENCY NOISE SPECTROSCOPY OF LASER DIODES

Richard Pinkrah

Summary

A comprehensive investigation of low-frequency noise characteristics of GaAs and GaAsBi based infrared laser diodes with parabolic and rectangular quantum wells were carried out. The aim of the investigation was to characterize the performance and quality of the lasers, to clear up noise origins in their structures.

The investigated laser diodes were grown by molecular beam epitaxy. Measured characteristics include current-voltage characteristics and light output power (operating characteristic), low-frequency (10 Hz – 20 kHz) optical and electrical noise properties, and cross-correlation factor between optical and electrical fluctuations. Measurements were carried out at room temperature and in temperature range from 88 K to 300 K for PQW lasers.

Current-voltage characteristic of the investigated laser diodes do not deviate far from the ideal behavior: the non-ideality factor of current-voltage characteristic is between 1 and 2. The flowing current mainly consists of diffusion and generation and recombination current components.

In low frequency noise characteristics, $1/f$ noise and generation and recombination fluctuations with Lorentzian spectrum are manifested. Presence of $1/f$ noise is caused by the superposition processes of generation and recombination of charge carrier. These generation and recombination carriers' centers are formed by different defects, dislocations, and imperfections in the active region of the laser diode structure. Electrical noise intensity for GaAsBi laser diode is very high as compared with GaAs rectangular and parabolic quantum well lasers due to larger number of defects caused by introduction of bismuth.

Cross-correlation factor between optical and electrical fluctuations shows a high positive correlation of optical and electrical, what indicates that there are defects in the active region of investigated laser diodes which control current flow through the active region.

Noise spectra at different temperatures were modeled and fitted by superposition of thermal noise, $1/f^{\alpha}$, $1/f$ and two Lorentzian components. The activation energy of observed two generation and recombination processes was evaluated and obtained 16.0 meV and 20.4 meV.

Results showed that low frequency noise characteristics of the investigated laser diodes do not depend on the quantum well profile (rectangular or parabolic), but noise intensity is larger for GaAsBi based devices.

Lazerinių diodų žemo dažnio triukšminė spektroskopija

Richard Pinkrah

Santrauka

Šiame darbe pristatomas infraraudonosios srities lazerinių diodų su GaAs ir GaAsBi parabolinėmis ir stačiakampėmis kvantinėmis duobėmis žemo dažnio triukšmo charakteristikų tyrimas. Tyrimo tikslas – ištirti šių lazerinių diodų veikimo charakteristikas ir kokybę, išsiaiškinti triukšmo šaltinius jų dariniuose.

Tirti lazeriniai diodai buvo auginami molekulinio pluošto epitaksijos būdu. Tirtos charakteristikos: voltamperinės ir spinduliuotės galios charakteristikos, žemo dažnio (10 Hz – 20 kHz) optinio ir elektrinio triukšmo priklausomybės, abipusė koreliaciją tarp optinių ir elektrinių fliuktuacijų. Matavimai buvo atlikti kambario temperatūroje ir temperatūros intervale nuo 88 K iki 300 K.

Tirtų lazerinių diodų voltamperinė charakteristika nedaug nukrypsta nuo idealios: voltamperinės charakteristikos neidealumo koeficientas yra tarp 1 ir 2. Tekančią srovę daugiausia sudaro difuzijos beigeneracinė ir rekombinacinį srovės komponentės.

Žemo dažnio triukšmo charakteristikose stebimas $1/f$ triukšmas bei generacinės ir rekombinacinės fliuktuacijos, kurioms būdingas Lorenco tipo spektras. $1/f$ triukšmą sukelia krūvininkų generacijos ir rekombinacijos vyksmų superpozicija. Šiuos krūvininkų generacijos ir rekombinacijos centrus kuria įvairūs defektai, dislokacijos ir kiti netobulumai aktyviojoje lazerinio diodo srityje. GaAsBi lazerinio diodo elektrinio triukšmo intensyvumas yra labai didelis, palyginti su GaAs lazeriais, dėl didesnio defektų skaičiaus, atsiradusių dėl bismuto įvedimo.

Abipusės koreliacijos koeficientas tarp optinių ir elektrinių fluktuacijų rodo didelę teigiamą optinio ir elektrinio koreliaciją: tiriamų lazerinių diodų darinyje yra defektų, valdančių srovės tekėjimą per aktyviąją sritį.

Elektrinio triukšmo spektrai esant skirtingai temperatūrai buvo aproksimuoti šiluminio triukšmo, $1/f^{\alpha}$, $1/f$ ir dviejų Lorenco komponenčių superpozicija. Buvo įvertinta dviejų aktyvių krūvininkų generacijos ir rekombinacijos procesų aktyvacijos energija, kuri yra 16,0 meV ir 20,4 meV.

Parodyta, kad tirtų lazerinių diodų žemo dažnio triukšmo charakteristikos nepriklauso nuo kvantinių duobių profilio (stačiakampio ar parabolinio), tačiau triukšmo intensyvumas yra didesnis lazeriniuose dioduose su GaAsBi kvantiniais dariniais

References

[1] R. N. Hall, G. E. Fenner, J. Kingsley, T. J. Soltys, and R. O. Carlson, *Phys. Rev. Lett.*, 9, 366 (1962).

[2] K. Oe and H. Okamoto, New semiconductor alloy GaAs1-xBix grown by metal organic vapor phase epitaxy, Jpn. J. Appl. Phys. 37-2(11A), L1283– L1285 (1998)

[3] Glemža, J., Palenskis, V., Geižutis, A., Čechavičius, B., Butkutė, R., Pralgauskaitė, S., and Matukas, J. Low-Frequency Noise Investigation of 1.09 μm GaAsBi Laser Diodes. Materials 2019, 12, p. 673. DOI: 10.3390/ma12040673

[4] L. K. J. Vandamme, Noise as a Diagnostic Tool for Quality and Reliability of Electronic Devices", IEEE Transactions on Electron Devices, Vol. 41. No 11, (1994), http://dx.doi.org/10.1109/16.333839

[5] Mawst L.J., Bhattacharya A., Lopez J., Botez D., Garbuzov D.Z.,DeMarco L., Connolly J.C., Jansen M., Fang F., Nabiev R.F. Appl. Phys. Lett., 69, 1532 (1996).

[6] Margi Sasono; Hariyadi Soetedjo (2010). A design of simple, portable optical tomography apparatus using 904 nm NIR laser diode., 121(15), 1418–1422.

[7] Phillips A F, Sweeney S J, Adams A R and Thijs P J A 1999 The temperature dependence of 1.3 μm and 1.5 μm compressively strained InGaAs(P) MQW semiconductor lasers IEEE J. Sel. Top. Quantum Electron. 5 401

[8] G.Bauer, G. Springholz, in Encyclopedia of Modern Optics 2005 Semiconductor Materials / Lead salt Pages 385-392

[9] S.M. Rezende Introduction to Electronic Materials and Devices, Optoelectronic Materials and Devices pp 261–344

[10] Stephan W Koch, Martin R. Hofmann, in Encyclopedia of Modern Optics (Second Edition), 2018

[11] Miller D A B, 1990a, Optoelectronic applications of quantum wells, Optics and Photonics News Vol. 1, No. 2 (February 1990)

[12] Renk, Karl F. (2012). [Graduate Texts in Physics] Basics of Laser Physics Volume 24 Quantum Wire and Quantum Dot Laser

[13] Diederik Aerts (1995). Quantum structures: An attempt to explain the origin of their appearance in nature. International Journal of Theoretical Physics, 34(8), 1165–1186.

[14] N.N. Ledentsov, M. Grundmann, F.Heinrichsdorff,D.Bimberg,V.M.Ustinov,A.E.

Zhukov,M. V. Maximov Z. I. Alferov, and J. A. Lott, “Quantum-Dot Heterostructure Lasers," *IEEE J. Selected* Topics *Quan. Elect.,* **6**, 439 (2000).

[15] Ridene, Said (2018). GaSbBi/GaSb quantum-well and wire laser diodes. Chemical Physics Letters, 702(), 44–48.

[16] Davydov VY, Averkiev NS, Goncharuk IN, Nelson DK, Nikitina IP. Raman and photoluminescence studies of biaxial strain in GaN epitaxial layers grown on 6H–SiC. J Appl Phys 1997; 82:5097–102.

[17] Perry WG, Zheleva T, Bremser MD, Davis RF, Shan W, Song JJ. Correlation of biaxial strains, bound exciton energies, and defect microstructures in GaN films grown on AIN/6H-SiC (0 00 1) substrates. J Electron Mater 1997;26: 224–31.

[18] Ma YY, Sudharsanam K, Pamidighantam R, Ishimura E. Design for enhancing reliability of LD chip in a 10 Gps optoelectronic package. IEEE Electron Package Technol Conf 2002:164–9.

[19] Lisak D, Cassidy DT, Moore AH. Bonding stress and reliability of high-power GaAs-based lasers. IEEE Trans Common Package Technology 2001; 24:92–8.

[20] Kuo CP, Vong SK, Cohen RM, Stringfellow GB. Effect of mismatch strain on band gap in III–V semiconductors. J Appl Phys 1985; 57:5428–32.

[21] Olsen GH, Nuese CJ, Smith RT. The effect of elastic strain on energy band gap and lattice parameter in III–V compounds. J Appl Phys 1978; 49:5523–9.

[22] R. Butkute, ˙ V. Pacebutas, B. Cechavi ˇ ˇcius, R. Nedzinskas, A. Selskis, A. Arlauskas, and A. Krotkus, Photoluminescence at up to 2.4 μm wavelengths fromGaInAsBi/ AlInAs quantum wells, J. Cryst.Growth391 (2014) 116-120.

[23] Cho A Y, 1991, Advances in molecular beam epitaxy (MBE) Journal of Crystal Growth Vol. 111

[24] Furuya K, and Miyamoto Y, 1990, GaInAsP/InP organometallic vapor phase epitaxy for research and fabrication of devices, Int. J. High Speed Electronics Vol. 1 347.

[25] Guo K X and Gu S W 1993 Phys. Rev. B 47 16322–16325

[26] Huang Y and Lien C 1994 J. Appl. Phys. 75 3223–3225

[27] Deimert, C., Wasilewski, Z.R. (2019). MBE growth of continuously graded parabolic quantum well arrays in AlGaAs. Journal of Crystal Growth, 514(), 103–108.

[28] H. Nyquist, Thermal Agitation Electric Charge in Conductors," Phys Rev 32, 110-113, (1928), http://dx.doi.org/10.1103/PhysRev.32.110

[29] B. K. Jones, Electrical noise as a reliability indicator in electronic devices and components, IEE Proc.-Circuits Devices Syst., Vol 149, No. 1, (2002), http://dx.doi.org/10.1049/ip-cds:20020331

[30] Jones, B.K: 'The scale invariance of 1/f noise. Proceedings of Unsolved problems of noise fluctuations, Adelaide, July 1999 pp.115-123

[31] Van der Ziel, "Unified presentation of 1/f noise in electronic devices: Fundamental 1/f noise sources," Proc. IEEE, vol. 76, p. 233, 1988

[32] F. N. Hooge and L. K. J. Vandamme, "Lattice scattering cause 1/f noise," Phys. Lett. A vol. 66, p. 315, 1978

[33] https://www.eng.auburn.edu/~wilambm/pap/2011/K10147_C011.pdf

[34] Brian K. Jones, Low-Frequency Noise spectroscopy, IEEE Transactions on electronic devices, Vol 41, No. 11. (1994), http://dx.doi.org/10.1109/16.333840

[35] M. Fukuda, Reliability and Degradation of Semiconductor Lasers and LEDs, Artech House, Inc., Norwood, MA 1991.

[36] O. Ueda, Reliability and Degradation of III-V Optical Devices, Artech House, Inc., Norwood, MA 1996.

[37] J. Wang, L. Bao, M. Devito, D. Xu, D. Wise, M. Grimshaw, W. Dong, S. Zhang, C. Bai, P. Leisher, D. Li, H. Zhou, S. Paterson, R. Martinsen and J. Haden, "Reliability and Performance of 808nm Single Emitter Multi-mode Laser Diodes", SPIE proceedings, Photonics West (2010)

[38] M. Vanzi, A. Bonfiglio, F. Magistrali, G. Salmini, Electron microscopy of life tested semiconductor laser diodes, Micron. 31 (2000) 259.

[39] H. C. Casey, Jr and M. B. Panish, Heterostructure Lasers (academic Press, New York, 1978), Vol. 1, p 44.

[40] Nunoya, N. et al. (2000). Sub-milliampere operation of 1.55μm wavelength high index coupled buried heterostructure distributed feedback lasers. Electronic letters, Vol. 36, No 14, (July 2000), pp. 1213-1214, ISSN 0013-5194.

[41] Lien CD, So FCT, Nicolet MA (1984). 'An Improved Forward I–V Method for Non-Ideal Schottky Diodes with High Series Resistance.' IEEE Trans. Electron Dev. ED-31:1502-1503.

[42] Pralgauskaite, S.; Palenksis, V.; Matukas, J. Chapter 8: Low frequency noise characteristics of multimode and ˙ singlemode laser diodes. In Semiconductor Laser Diode Technology and Applications; Patil, D.S., Ed.; InTech: London, UK, 2012; ISBN 978-953-51-0549-7. pp. 133–160.

[43] V. Palenskis, J.Matukas, S Pralgauskaité and B. Saulys, A detail analysis of optical fluctuations of green light emitting diodes by correlation method, Fluctuation Noise Lett 9, 179-192 (2010)

[44] Armalytė, S., Glemža, J., Jonkus, V., Pralgauskaitė, S., Matukas, J., Pūkienė, S., ... & Butkutė, R. (2023). Low-frequency noise characteristics of (Al, Ga) As and Ga (As, Bi) quantum well structures for NIR laser diodes. *Sensors*, *23*(4), 2282.